# Interplay between Magnetism, Superconductivity, and Orbital Order in 5-Pocket Model for Iron-Based Superconductors: Parquet Renormalization Group Study

Laura Classen,[1,2] Rui-Qi Xing,[2] Maxim Khodas,[3,4] and Andrey V. Chubukov[2]
[1]*Institut für Theoretische Physik, Universität Heidelberg, 69120 Heidelberg, Germany*
[2]*School of Physics and Astronomy, University of Minnesota, Minneapolis, Minnesota 55455, USA*
[3]*Department of Physics and Astronomy, University of Iowa, Iowa City, Iowa 52242, USA*
[4]*Racah Institute of Physics, The Hebrew University, Jerusalem 91904, Israel*
(Received 5 August 2016; published 20 January 2017)

We report the results of the parquet renormalization group (RG) analysis of the phase diagram of the most general 5-pocket model for Fe-based superconductors. We use as an input the orbital structure of excitations near the five pockets made out of $d_{xz}$, $d_{yz}$, and $d_{xy}$ orbitals and argue that there are 40 different interactions between low-energy fermions in the orbital basis. All interactions flow under the RG, as one progressively integrates out fermions with higher energies. We find that the low-energy behavior is amazingly simple, despite the large number of interactions. Namely, at low energies the full 5-pocket model effectively reduces either to a 3-pocket model made of one $d_{xy}$ hole pocket and two electron pockets or a 4-pocket model made of two $d_{xz}/d_{yz}$ hole pockets and two electron pockets. The leading instability in the effective 4-pocket model is a spontaneous orbital (nematic) order, followed by $s^{+-}$ superconductivity. In the effective 3-pocket model, orbital fluctuations are weaker, and the system develops either $s^{+-}$ superconductivity or a stripe spin-density wave. In the latter case, nematicity is induced by composite spin fluctuations.

DOI: 10.1103/PhysRevLett.118.037001

*Introduction.*—The interplay between superconductivity, magnetism, and nematicity is the key physics of Fe-based superconductors (FeSCs) [1–6]. In some FeSCs, e.g., 1111 and 122 systems, undoped materials display a stripe magnetic order below a certain $T_N$ and a nematic order at slightly higher temperatures, while superconductivity emerges upon doping, when magnetic order gets weaker. In other systems, like 111 LiFeAs and 11 FeSe, superconductivity emerges without long-ranged magnetism already in undoped systems. Besides, FeSe displays an orbital order above the superconducting (SC) $T_c$ [7]. The issue for the theory is to understand whether these seemingly different behaviors can be understood within the same framework.

In this Letter, we report the results of our analysis, which connects different classes of FeSCs. We study the competition between superconductivity, magnetism, and nematicity in the most generic five-pocket ($5p$) model for FeSCs with full orbital content of low-energy excitations. To do this, we use the machinery of the analytical parquet renormalization group (pRG) [8]. This approach, along with the complementary numerical functional RG [9–12], has been argued [4,9–16] to be the most unbiased way to analyze competing orders in an itinerant electron system.

The $5p$ model consists of three hole pockets, of which two are centered at $\Gamma = (0, 0)$ in the 1Fe Brillouin zone and one is centered at $M = (\pi, \pi)$, and two electron pockets centered at $Y = (0, \pi)$ and $X = (\pi, 0)$ (see the right panel in Fig. 1). The two $\Gamma$-centered hole pockets are made out of $d_{xz}$ and $d_{yz}$ orbitals, and the hole pocket at $M$ is made out of $d_{xy}$ orbitals. The electron pockets are made out of $d_{xz}(d_{yz})$ and $d_{xy}$ orbitals [17,18].

For such an electronic configuration, there are 40 different four-fermion interaction terms, allowed by $C_4$ symmetry [19,20] (without the hole pocket at $M$, this number is 30 [21]). If one departs from the model with only local interactions, the bare values of all 40 interactions are linear combinations of Hubbard and Hund terms. However, the 40 interactions flow to different values under the pRG, which implies that the system self-generates nonlocal interactions. The flow of the interactions is obtained by solving differential equations that encode a series of coupled vertex renormalizations. The running interactions are then used as input to determine susceptibilities in different channels. This way one can monitor a simultaneous buildup of different correlations taking into account their mutual feedback, which turns out to be crucial in our study.

The main result of pRG analysis is the emergent universality. It means that 40 microscopic interactions flow towards a *limited number* of fixed trajectories (FTs), where the ratios of different interactions become universal numbers. Each fixed trajectory has a basin of attraction in the space of bare interaction parameters. This allows us to explain the rich behaviors of the different FeSCs within a unifying description. In practical terms, a simultaneous buildup of different correlations holds in the window of energies between a fraction of $W$ and a scale comparable to the Fermi energy $E_F$. At smaller energies, interactions in different channels evolve independently of each other.

 

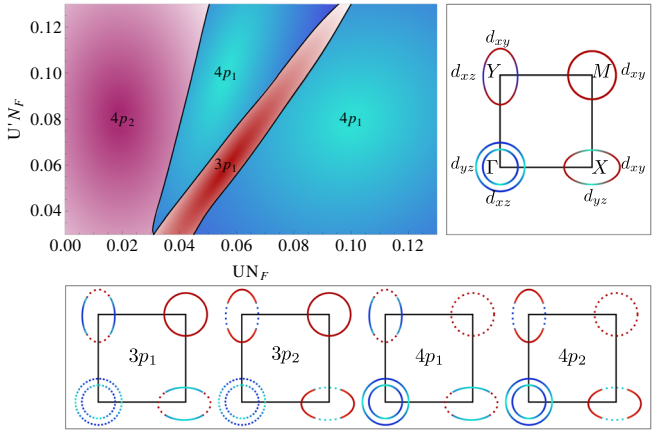


FIG. 1. (Upper panel) Right: main orbital content of excitations near Fermi surfaces (presented by different colors); left: regions of different system behavior of the full 5-pocket model, indicated by the type of the effective model. In the ranges marked $4p_{1,2}$, the dominant interactions are between fermions near the Γ-centered hole pockets and electron pockets. In the regions $3p_{1,2}$, the dominant interactions at low energies are within the subset of the two electron pockets and the $M = (\pi, \pi)$-hole pocket. The index 1,2 distinguishes if interactions involving $d_{xz}/d_{yz}$ or $d_{xy}$ orbital components on the electron pockets are dominant. For illustration purposes, we used the bare model with local Hubbard and Hund interactions—intraorbital $U$, interorbital $U'$, $J$, and $J'$. We set $J = 0.025/N_F$ and $J' = 0.03/N_F$, where $N_F$ is the density of states on the FSs (assumed to be equal on all FSs for simplicity), and varied $U$ and $U'$ as two independent parameters. For this particular choice, $3p_2$ region does not exist. (Lower panel) Graphic representations of $3p_{1,2}$ and $4p_{1,2}$ models. Fermionic states, for which interactions become the largest in the process of pRG flow, are shown by solid lines.

The range between $W$ and $E_F$ should be wide enough; otherwise, the pRG flow ends before the system reaches one of the FTs [22].

*Summary of our results.*—We found four stable FTs. For the first two stable FTs, the interactions within the subset of the two Γ-centered hole pockets and the two electron pockets become dominant; i.e., the $5p$ model effectively reduces to the four-pocket model ($4p$). For the other two stable FTs, the $5p$ model reduces to an effective 3-pocket model ($3p$) consisting of two electron pockets and the $M$-hole pocket. On each of two stable $4p$ FTs or $3p$ FTs, the system behavior is described by an even simpler effective model, because interactions involving fermions from either $d_{xz}/d_{yz}$ or $d_{xy}$ orbitals become dominant. We label these models as $4p_1$, $3p_1$ and $4p_2$, $3p_2$, respectively. We illustrate the four cases and present the phase diagram in Fig. 1. We then computed susceptibilities in different channels [23]. We found that the interplay between spin-density-wave (SDW) magnetism and superconductivity is the same in all four effective models. Namely, the SDW susceptibility is the largest at intermediate energies and pushes SC and orbital susceptibilities up. However, in the process of the pRG flow, the SC susceptibility overtakes the SDW one, and the feedback from SC fluctuations halts the increase of the SDW susceptibility [see Fig. 3(b)]. As a consequence, already the undoped system develops superconductivity rather than SDW magnetism, if indeed the pRG flow runs over a wide enough range of energies. This result could not be obtained within the RPA and is entirely due to the feedback from increasing SC fluctuations on the SDW channel. In all cases, superconductivity is of the $s^{+-}$ type, with a sign change between the gaps on hole and electron pockets. In $4p$ models, the susceptibility towards $C_4$-breaking orbital order also grows, and its exponent is larger than that for superconductivity [4]; i.e., the system first develops a spontaneous orbital order. In $3p$ models, orbital fluctuations are much weaker, and orbital order does not have enough "space" to develop.

We found that SDW magnetism does develop before superconductivity and/or orbital order if the FT is not reached within the range of pRG flow. The type of SDW order is different for the $3p$ and the $4p$ models. In $3p$ models SDW order is a $C_4$-breaking stripe order [24,25], while in $4p$ models it is $C_4$-preserving double-$Q$ order [26,27] [a symmetric combination of $(\pi, 0)$ and $(0, \pi)$ magnetic orders]. This last result, in combination with the pRG, implies a clear separation between the magnetic and orbital scenario for nematicity in FeSCs. Namely, in $4p$ models, the SDW scenario for Ising-nematic order does not work, because double-$Q$ SDW preserves the symmetry between the $X$ and $Y$ directions, and, simultaneously, orbital fluctuations are strong. In $3p$ models, orbital fluctuations are weak, and, simultaneously, SDW *stripe* fluctuations favor vestigial Ising-nematic spin order [28].

In the remainder of this Letter, we present the details of our study. The full analysis of the set of 40 pRG equations is quite involved, so, to demonstrate the separation into $4p$ or $3p$ behavior at low energies, we first analyze a toy model, in which we approximate the orbital composition of the two electron pockets as pure $d_{xy}$. We then extend the analysis to the full 5-pocket model.

*Toy model with $d_{xy}$ electron pockets.*—As we said, the kinetic term describes fermionic excitations around the five Fermi surfaces, i.e., $H = H^{\Gamma} + H^{X} + H^{Y} + H^{M}$. The symmetry-allowed interaction terms contain 14 interactions $U_i$ within the subset of the two electron and the two Γ-centered hole pockets and seven interactions $U_{\text{in}}$ involving fermions near the $M$-hole pocket, so the total number of the interactions is 21. We present the Hamiltonian and the full set of pRG equations for a generic dispersion near hole and electron FSs in Supplemental Material [20]. The pRG analysis shows that six interactions flow to zero and five increase with smaller exponents than the other ten. The pRG flow of the remaining ten interactions determines the FTs. We show these ten interactions in the inset in Fig. 3(a). The pRG equations for these interactions are ($u_i = U_i N_F$)

$$\dot{u}_1 = u_1^2 + u_3^2, \qquad \dot{u}_{1n} = u_{1n}^2 + u_{3n}^2,$$
$$\dot{u}_2 = 2u_2(u_1 - u_2), \qquad \dot{u}_{2n} = 2u_{2n}(u_{1n} - u_{2n}),$$
$$\dot{u}_3 = 2u_3(2u_1 - u_2 - u_5) - 2u_3u_4 - u_{3n}u_{5n},$$
$$\dot{u}_{3n} = 2u_{3n}(2u_{1n} - u_{2n} - u_5) - u_{3n}u_{4n} - 2u_3u_{5n},$$
$$\dot{u}_4 = -2u_4^2 - 2u_3^2 - 2u_{5n}^2, \qquad \dot{u}_{4n} = -u_{4n}^2 - 2u_{3n}^2 - 2u_{5n}^2,$$
$$\dot{u}_5 = -2u_5^2 - 2u_3^2 - u_{3n}^2,$$
$$\dot{u}_{5n} = -2u_4u_{5n} - u_{4n}u_{5n} - 2u_3u_{3n}. \quad (1)$$

The derivatives are with respect to $L = \log W/E$, where $E$ is the running scale.

We searched for FTs of Eq. (1) by selecting one divergent interaction (specifically, $u_1$ or $u_{1n}$), writing other interactions as $u_i = \gamma_i u_1$, $u_{\rm in} = \gamma_{\rm in} u_1$ (or $u_i = \gamma_i u_{1n}$, $u_{\rm in} = \gamma_{\rm in} u_{1n}$), and solving the set of equations for $L$-independent $\gamma_i$, $\gamma_{\rm in}$. We found two stable FTs: one with

$$u_1 = \frac{1}{1+\gamma_3^2}\frac{1}{L_0 - L}, \quad (2)$$

$\gamma_{\rm in} = \gamma_2 = 0$, $\gamma_3 = \pm\sqrt{15}$, and $\gamma_4 = \gamma_5 = 3$, and the other with

$$u_{1n} = \frac{1}{1+\gamma_{3n}^2}\frac{1}{L_0 - L}, \quad (3)$$

$\gamma_1 = \gamma_2 = \gamma_3 = \gamma_4 = \gamma_{2n} = \gamma_{5n} = 0$, $\gamma_{3n} = \pm(3 + 2\sqrt{6})$, and $\gamma_{4n} = 2\gamma_5 = -\sqrt{6}$. In Eqs. (2) and (3), $L_0$ is the scale at which interactions diverge and the system develops a long-range order, as we show below. For the first stable FT, all $\gamma_{\rm in}$ involving the $M$ pocket vanish, so the 5-pocket model effectively reduces to the $4p$ model. For the second stable FT, the situation is the opposite—interactions involving the two $\Gamma$-centered hole pockets vanish compared to other interactions; i.e., the $5p$ model effectively reduces to the $3p$ model. We checked the stability of the $4p$ FT and the $3p$ FT by expanding around them and verified that all eigenvalues are negative. Whether the system flows to one FT or the other is determined by the bare values of the interactions (see Fig. 2).

We next use the running interactions as inputs and compute the susceptibilities in different channels, $\chi_j$. We describe the computational procedure in Ref. [20] and here list the results. The potentially divergent parts of the susceptibilities in SC and SDW channels are $\chi_i \propto (L_0 - L)^{2\beta_i - 1}$ ($i$ = SDW, SC). Along $4p$ FT and $3p$ FT, the exponents are $\beta_{\rm SDW}^{(4p)} = 0.30$, $\beta_{\rm SC}^{(4p)} = 0.86$, $\beta_{\rm SDW}^{(3p)} = 0.43$, and $\beta_{\rm SC}^{(3p)} = 0.72$. We see that in both cases $\beta_{\rm SC} > 1/2$ while $\beta_{\rm SDW} < 1/2$; i.e., $\chi_{\rm SC}$ diverges at $L = L_0$, while $\chi_{\rm SDW}$ remains finite, despite that it was the largest at the beginning of the pRG flow. This implies that the system develops SC order but not SDW order. We show the flow of the susceptibilities in Fig. 3(b). For both $4p$ and $3p$ models, we found that the largest $\beta_{\rm SC} > 0$ corresponds to the $s^{+-}$ gap structure, with the opposite sign of the gap on the hole and electron pockets [29]

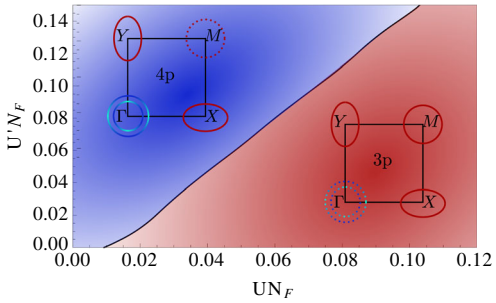


FIG. 2. Two different regions of system behavior indicated by fixed trajectories of the pRG flow for the toy model with electron pockets made entirely of $d_{xy}$, for different values of $U$, $U'$ (treated as two independent parameters) and $J = J' = 0.03/N_F$. In the region labeled as $3p$, the interactions within the subset of the two electron pockets and the $M = (\pi, \pi)$-hole pocket become dominant at low energies. In the region labeled as $4p$, interactions involving fermions from the two $\Gamma$-centered hole pockets and the two electron pockets become dominant.

We also analyzed the susceptibility $\chi_P$ in the $d$-wave Pomeranchuk channel. An instability in this channel leads to spontaneous orbital order [4,6], i.e., nonequal densities of fermions on $d_{xz}$ and $d_{yz}$ orbitals. For the $4p$ model, we found that $\beta_P^{(4p)} = 1$ is larger than $\beta_{\rm SC}^{(4p)}$; i.e., orbital order can precede the SC transition [4]. We found no $d_{xz}/d_{yz}$ orbital order for the $3p$ model, because the electron and the $M$ pockets have $d_{xy}$ character [30].

*Full 5-pocket model.*—The analysis of the full 5-pocket model with $d_{xz}/d_{xy}$ and $d_{yz}/d_{xy}$ orbital content of the electron pockets is more involved, as one has to analyze the set of 40 coupled differential equations for the interactions (see [20]). We searched for FTs with the same procedure as in the toy model. Amazingly enough, we found much the same behavior. Namely, the $5p$ model effectively becomes either a $4p$ or a $3p$ model. The new feature, not present in the toy model, is that in each case there are now two stable FTs, on which the system behavior is described by even more restricted $3p_{1,2}$ and $4p_{1,2}$ models. For $3p_1$ and $4p_1$ models, interactions involving fermions from $d_{xz}$ ($d_{yz}$) orbitals on the electron pockets become dominant; for $3p_2$ and $4p_2$ models, interactions of $d_{xy}$ orbitals on the electron pockets become dominant. We verified that these four FTs are stable with respect to small deviations. We show the phase diagram in Fig. 1.

The interplay between SDW and SC is the same in all four effective models and is similar to that in the toy model. Namely, the SDW susceptibility is the largest at the beginning, but in the process of the flow SC susceptibility diverges faster, and the feedback from SC fluctuations halts the growth of SDW susceptibility. As a

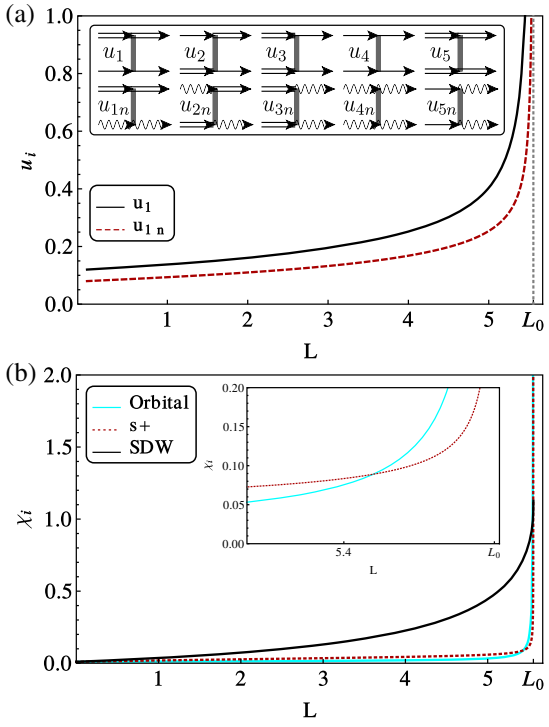


FIG. 3. (a) Representative RG flow towards the $4p$ FT in the toy model for the interactions $u_1$ and $u_{1n}$. The inset shows the ten relevant interactions of the toy model, where double lines represent electron pockets, wavy lines the $M$-centered hole pocket, and solid single lines the Γ-centered hole pockets. Bare values are $U=0.08/N_F$, $U'=0.12/N_F$, and $J=J'=0.03/N_F$. The RG parameter $L$ is $\log W/E$, where $W$ is the bandwidth and $E$ is running energy or temperature. The system undergoes an instability into an ordered state (SDW, SC, or orbital order) at $L=L_0$. (b) Corresponding flow of the SDW, SC $s^{+-}$ and orbital susceptibilities. Near $L=L_0$, the SC and the orbital susceptibilities keep increasing, while the SDW susceptibility remains finite. Inset: Orbital and SC susceptibilities near the end of the flow.

result, even at zero doping the system develops $s^{+-}$ SC order but no SDW order. Orbital fluctuations are, however, different in $4p$ and $3p$ models, again in similarity to the toy model. If the pRG flow is towards $4p_1$ or $4p_2$ models, orbital fluctuations also get strong and $\chi_P$ diverges with the largest exponent; i.e., the system develops a spontaneous orbital order prior to SC [32]. If the flow is towards the $3p$ model, orbital fluctuations are much weaker and do not develop for not too large $W/E_F$. If $E_F$ is larger than $E_0 \sim We^{-L_0}$, the pRG flow ends before $\chi_{SC}$ and/or $\chi_P$ wins over $\chi_{SDW}$. In this situation, the system develops SDW order at smaller doping and SC order at larger dopings [22]. For the $4p$ model an SDW order is a double-$Q$ order, maintaining the symmetry between $X$ and $Y$ directions [26,27], while for the $3p$ model SDW order is a stripe, breaking this symmetry [24,25]. Combining this with pRG results, we find that, if the pRG flow is towards one of the two $4p$ models, the nematicity emerges as a spontaneous orbital order. If the flow is towards one of the $3p$ models, the nematicity emerges due to stripe fluctuations as a composite Ising-nematic spin order.

*Conclusions and applications to FeSCs.*—In this Letter, we analyzed the competition between SDW, SC, and orbital order in the full 5-pocket model for FeSCs. We used pRG techniques and included into consideration the orbital composition of hole and electron pockets in terms of $d_{xz}$, $d_{yz}$, and $d_{xy}$ orbitals. We found that the system behavior is amazingly simple—depending on the initial values of the interactions and quasiparticle masses, the system flows to one of four stable FTs. For two of these FTs, the system behavior at low energies is the same as if the $M$-pocket was absent ($4p$ model); for the other two, the system behavior is the same as if the two Γ-centered hole pockets were absent ($3p$ model).

Our results have several implications for FeSCs. First, the pRG analysis shows that SC order may develop instead of long-ranged magnetism already in undoped materials, not only when SDW order is destroyed by doping. This is consistent with the behavior in LiFeAs and FeSe [33]. In systems with smaller regions of the pRG flow (larger bare interactions or larger $E_F$), SDW order develops first, and SC develops only upon doping. Second, pRG analysis shows that in $4p$ models orbital order develops first, SC develops at a lower $T$, and SDW order does not develop down to $T=0$. This is consistent with the observed behavior in FeSe at ambient pressure [7]. Third, in $4p$ models nematicity is due to orbital order, while in the $3p$ model it is of magnetic origin (composite Ising-nematic order). Whether the system flows towards a $3p$ or $4p$ effective model at low energies depends on microscopic interactions (see Figs. 1 and 2) as well as the parameters of fermionic dispersions (see [20]).

The phase diagram in Fig. 1 describes the behavior found in all four families of FeSCs—1111, 122, 111, and 11 systems—and in this respect our findings provide a unified description of the competition between SDW, SC, and orbital orders in all FeSCs.

We acknowledge with thanks the discussions with E. Berg, L. Boeri, S. Borisenko, P. Coleman, R. Fernandes, C. Honerkamp, D.-H. Lee, W. Metzner, A. Nevedomsky, D. Podolsky, M. Scherer, Q. Si, R. Thomale, A.-M. Tremblay, O. Vafek, C. Varma, and Fa Wang. L. C. thanks the School of Physics and Astronomy of the University of Minnesota for hospitality during this work and acknowledges funding by the Studienstiftung des deutschen Volkes and the HGSFP at Heidelberg University. A. V. C. is supported by the Office of Basic Energy Sciences, U.S. Department of Energy, under Award No. DE-SC0014402. M. K. is supported by the Israel Science Foundation ISF, Grant No. 1287/15 and NSF DMR-1506668.

[1] R. M. Fernandes, A. V. Chubukov, and J. Schmalian, Nat. Phys. **10**, 97 (2014); P. C. Canfield and S. L. Bud'ko, Annu. Rev. Condens. Matter Phys. **1**, 27 (2010).

[2] S. Liang, A. Moreo, and E. Dagotto, Phys. Rev. Lett. **111**, 047004 (2013).

[3] See, e.g., A. V. Chubukov, in *Iron-based Superconductivity*, Springer Series in Materials Science Vol. 211 (Springer, New York, 2015), pp. 255–329; L. de' Medici, *ibid*, pp. 409–441.

[4] A. V. Chubukov, M. Khodas, and R. M. Fernandes, Phys. Rev. X **6**, 041045 (2016).

[5] V. Cvetkovic and Z. Tesanovic, Phys. Rev. B **80**, 024512 (2009).

[6] H. Yamase and R. Zeyher, Phys. Rev. B **88**, 180502(R) (2013); C. C. Lee, W. G. Yin, and W. Ku, Phys. Rev. Lett. **103**, 267001 (2009); F. Kruger, S. Kumar, J. Zaanen, and J. van den Brink, Phys. Rev. B **79**, 054504 (2009); B. Valenzuela, E. Bascones, and M. J. Calderon, Phys. Rev. Lett. **105**, 207202 (2010); W. Lv and P. Phillips, Phys. Rev. B **84**, 174512 (2011); W-C. Lee and P. W. Phillips, Phys. Rev. B **86**, 245113 (2012); R. Applegate, R. R. P. Singh, C. C. Chen, and T. P. Devereaux, Phys. Rev. B **85**, 054411 (2012); V. Stanev and P. B. Littlewood, Phys. Rev. B **87**, 161122(R) (2013); P. T. Dumitrescu, M. Serbyn, R. T. Scalettar, and A. Vishwanath, Phys. Rev. B **94**, 155127 (2016); S.-H. Baek, D. V. Efremov, J. M. Ok, J. S. Kim, J. van den Brink, and B. Buchner, Nat. Mater. **14**, 210 (2015); I. Gallais and I. Paul, C.R. Phys. **17**, 113 (2016); Z. Wang and A. H. Nevidomskyy, J. Phys. Condens. Matter **27**, 225602 (2015); V. K. Thorsmolle, M. Khodas, Z. P. Yin, C. Zhang, S. V. Carr, P. Dai, and G. Blumberg, Phys. Rev. B **93**, 054515 (2016).

[7] M. D. Watson, T. K. Kim, A. A. Haghighirad, N. R. Davies, A. McCollam, A. Narayanan, S. F. Blake, Y. L. Chen, S. Ghannadzadeh, A. J. Schofield, M. Hoesch, C. Meingast, T. Wolf, and A. I. Coldea, Phys. Rev. B **91**, 155106 (2015); Y. Suzuki, T. Shimojima, T. Sonobe, A. Nakamura, M. Sakano, H. Tsuji, J. Omachi, K. Yoshioka, M. Kuwata-Gonokami, T. Watashige, R. Kobayashi, S. Kasahara, T. Shibauchi, Y. Matsuda, Y. Yamakawa, H. Kontani, and K. Ishizaka, Phys. Rev. B **92**, 205117 (2015); Y. Zhang *et al.*, arXiv: 1503.01556; P. Zhang *et al.*, Phys. Rev. B **91**, 214503 (2015); K. Kothapalli *et al.*, Nat. Commun. **7**, 12728 (2016); A. Fedorov, A. Yaresko, T. K. Kim, E. Kushnirenko, E. Haubold, T. Wolf, M. Hoesch, A. Gruneis, B. Buchner, and S. Borisenko (unpublished).

[8] See, e.g., A. T. Zheleznyak, V. M. Yakovenko, and I. E. Dzyaloshinskii, Phys. Rev. B **55**, 3200 (1997), and references therein.

[9] W. Metzner, C. Castellani, and C. Di Castro, Adv. Phys. **47**, 317 (1998); M. Salmhofer, Commun. Math. Phys. **194**, 249 (1998).

[10] C. Platt, C. Honerkamp, and W. Hanke, New J. Phys. **11**, 055058 (2009).

[11] C. Platt, W. Hanke, and R. Thomale, Adv. Phys. **62**, 453 (2013).

[12] F. Yang, F. Wang, and D. H. Lee, Phys. Rev. B **88**, 100504 (2013).

[13] K. LeHur and T. M. Rice, Ann. Phys. (Amsterdam) **324**, 1452 (2009).

[14] L. Nandkishore, L. Levitov, and A. V. Chubukov, Nat. Phys. **8**, 158 (2012); M. L. Kiesel, C. Platt, W. Hanke, D. A. Abanin, and R. Thomale, Phys. Rev. B **86**, 020507 (2012).

[15] A. V. Chubukov, D. V. Efremov, and I. Eremin, Phys. Rev. B **78**, 134512 (2008); D. Podolsky, H-Y. Kee, and Y. B. Kim, Europhys. Lett. **88**, 17004 (2009); S. Maiti and A. V. Chubukov, Phys. Rev. B **82**, 214515 (2010).

[16] Y. Yamakawa, S. Onari, and H. Kontani, Phys. Rev. X **6**, 021032 (2016).

[17] See, e. g., A. F. Kemper, T. A. Maier, S. Graser, H.-P. Cheng, P. J. Hirschfeld, and D. J. Scalapino, New J. Phys. **12**, 073030 (2010), and references therein.

[18] See, e. g., V. Brouet, M. F. Jensen, P. H. Lin, A. Taleb-Ibrahimi, P. Le Fevre, F. Bertran, C. H. Lin, W. Ku, A. Forget, and D. Colson, Phys. Rev. B **86**, 075123 (2012).

[19] The 40 interactions involve pairs of fermions, each pair near either the $\Gamma$, $X$, $Y$, or $M$ point. There are four additional interactions involving fermions near each of these points. These additional interactions do not affect the behavior near the four stable fixed trajectories that we found within the space of 40 couplings, as we explicitly verified. We neglect these additional interactions in our analysis.

[20] See Supplemental Material at http://link.aps.org/supplemental/10.1103/PhysRevLett.118.037001 for details.

[21] V. Cvetkovic and O. Vafek, Phys. Rev. B **88**, 134510 (2013) See also R. M. Fernandes and O. Vafek, Phys. Rev. B **90**, 214514 (2014).

[22] See, e. g., S. Maiti and A. V. Chubukov, Phys. Rev. B **82**, 214515 (2010) for a detailed explanation.

[23] A similar procedure has been used in the RG studies of other problems: see, e.g., W. Metzner, M. Salmhofer, C. Honerkamp, V. Meden, and K. Schoenhammer, Rev. Mod. Phys. **84**, 299 (2012), and references therein; Y. Lemonik, I. L. Aleiner, and V. L. Fal'ko, Phys. Rev. B **85**, 245451 (2012); J. M. Murray and O. Vafek, Phys. Rev. B **89**, 201110(R) (2014).

[24] I. Eremin and A. V. Chubukov, Phys. Rev. B **81**, 024511 (2010).

[25] P. Chandra, P. Coleman, and A. I. Larkin, Phys. Rev. Lett. **64**, 88 (1990); C. Fang, H. Yao, W-F. Tsai, J. P. Hu, and S. A. Kivelson, Phys. Rev. B **77**, 224509 (2008); C. Xu, M. Muller, and S. Sachdev, Phys. Rev. B **78**, 020501(R) (2008).

[26] R. M. Fernandes, M. Khodas, and A. V. Chubukov (to be published).

[27] M. N. Gastiasoro, I. Eremin, R. M. Fernandes, and B. M. Andersen, arXiv:1607.04711.

[28] R. M. Fernandes, A. V. Chubukov, J. Knolle, I. Eremin, and J. Schmalian, Phys. Rev. B **85**, 024534 (2012).

[29] For the $3p$ case, the subleading eigenfunction (smaller $\beta_{SC} > 0$) describes the orbital-antiphase state with the gap sign on the $M$ pocket opposite to that on the other four pockets; see Z. P. Yin, K. Haule, and G. Kotliar, Nat. Phys. **10**, 845 (2014).

[30] We call orbital order the symmetry breaking between $d_{xz}$ and $d_{yz}$ orbitals. Another $C_4$-symmetry-breaking term is the difference in the occupations of $d_{xy}$ orbitals at $X$ and $Y$ in the 1FeBZ [31]. Such an order is present in our $3p_2$ model and $4p_2$ models.

[31] R. M. Fernandes and O. Vafek, Phys. Rev. B **90**, 214514 (2014).
[32] For the application of the full $4p$ model to FeSe, see R. Xing, L. Classen, M. Khodas, and A. V. Chubukov, arXiv:1611.03912.
[33] SC not preceded by SDW already at zero doping has been detected in a fRG analysis of a 4-pocket model and contrasted with the reported lack of such a tendency in 5-pocket models [34]. We argue that the outcome of the pRG flow is qualitatively the same in both cases; only in the 5-pocket model the SC susceptibility overcomes the SDW susceptibility at smaller energies, i.e., after a longer RG flow.
[34] R. Thomale, C. Platt, W. Hanke, and B. A. Bernevig, Phys. Rev. Lett. **106**, 187003 (2011).